EDGE ARTICLE

Check for updates

Multiple rotational rates in a guest-loaded, amphidynamic zirconia metal–organic framework†

Aaron Torres-Huerta, [a] Dazaet Galicia-Badillo, [a] Andrés Aguilar-Granda, ‡[a] Jacob T. Bryant, [b] Fernando J. Uribe-Romo *[b] and Braulio Rodríguez-Molina *[a]

Amphidynamic motion in metal–organic frameworks (MOFs) is an intriguing emergent property, characterized by high rotational motion of the phenylene rings that are embedded within an open, rigid framework. Here, we show how the phenylene rings in the organic linkers of the water stable MOF PEPEP-PIZOF-2 exhibit multiple rotational rates as a result of the electronic structure of the linker, with and without the presence of highly interacting molecular guests. By selective ^2H enrichment, we prepared isotopologues PIZOF-2d_4 and PIZOF-2d_8 and utilized solid-state ^{13}C and ^2H NMR to differentiate the dynamic behavior of specific phenylenes in the linker at room temperature. A difference of at least one order of magnitude was observed between the rates of rotation of the central and outer rings at room temperature, with the central phenylene ring, surrounded by ethynyl groups, undergoing ultrafast 180° jumps with frequencies higher than 10 MHz. Moreover, loading tetracyanoquinodimethane (TCNQ) within the pores produced significant changes in the MOF's electronic structure, but very small changes were observed in the rotational rates, providing an unprecedented insight into the effects that internal dynamics have on guest diffusion. These findings would help elucidate the in-pore guest dynamics that affect transport phenomena in these highly used MOFs.

Amphidynamic crystals are an emerging class of materials made of molecular components that exhibit fast internal motion within a rigid lattice.[1,2] Metal–organic frameworks (MOFs) can be considered as intrinsically amphidynamic materials, because they are formed by the assembly of organic molecules that carry high degrees of freedom linked to inorganic clusters that form an extended solid matrix.[3] This assembly allows for the organic components to behave like rotators, while the solid matrix/framework acts as a stator, with gyroscope-type motion enabled by the open architecture of the MOF with motion modulated by the molecular structure of the linker.[4–6] In order to create materials with targeted dynamic properties for real-life applications, like molecular machines, it is important to determine whether the chemical environment of the linkers can produce dynamics at multiple rates and how the

presence of molecular guests affect such dynamics. To do so, it is important to use MOFs that are chemically stable to water and humidity, because this robustness increases the reproducibility of the results and the applicability of the MOF. The interplay between guest diffusion, linker dynamics and the overall framework flexibility has been actively investigated in recent years.[7]

Here, we prepared a water-stable MOF, **PEPEP-PIZOF-2** (Fig. 1a), strategically labelled with deuterium atoms to probe the multiple segmental motion in the pristine and guest-loaded materials. Utilizing solid-state NMR techniques, we elucidated that this MOF exhibits bimodal rotational rates, with the central ring of the linker having free rotation above the 10 MHz limit of quantitation, and with the outer rings having slower rotation. This double-rate internal dynamics is preserved even in the presence of a very "sticky," electron-deficient guest such as tetracyanoquinodimethane, TCNQ. Studying the molecular dynamics of this class of MOFs helps in accelerating their use as applied materials and for the fundamental studies of transfer phenomena that occur in MOFs such as mass, heat, and momentum transfer.

Zirconia MOFs have been shown to exhibit unprecedented chemical stability, of which the family of Porous Interpenetrated Zirconia Organic Frameworks (PIZOFs) features superior stability combined with a unique molecular composition of their linkers.[8,9] The linkers in PIZOF MOFs are linear and

[a]*Instituto de Química, Universidad Nacional Autónoma de México, Circuito Exterior, Ciudad Universitaria, 04510, Ciudad de México, Mexico. E-mail: brodriguez@iquimica.unam.mx*

[b]*Department of Chemistry and Renewable Energy and Chemical Transformations Cluster, University of Central Florida, 4111 Libra Drive, Room 251 PSB, 32816-2366, Orlando, Florida, USA. E-mail: fernando@ucf.edu*

‡ Current address: Department of Chemistry, University of Toronto, Toronto, ON M5S 3H6, Canada.
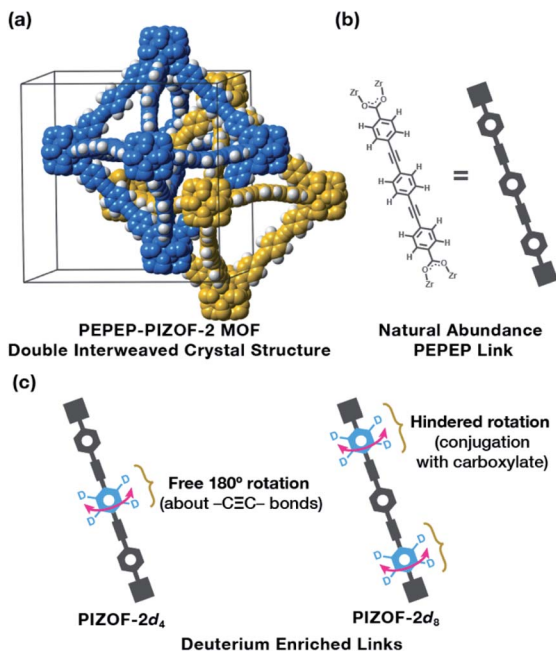
Fig. 1 (a) Crystal structure of the double interweaved MOF **PIZOF-2**, showing each framework in separate colors. (b) Molecular structure of the PEPEP link. (c) Deuterium enriched linkers used in this study emphasizing the deuterium location in the link and the different chemical environments.

made by a combination of phenylene rings and ethynylene groups, where multiple chemical environments can be created around the phenylenes, thus altering their rotational behavior. Of the series, **PEPEP-PIZOF-2** (hereafter **PIZOF-2**) is a high symmetry interweaved MOF (interweaved = interpenetrated with minimally displaced frameworks[10,11]) made with linkers that contain three phenylenes (P) and two ethynylenes (E) in an alternating form (hence PEPEP, Fig. 1b), creating two different types of chemical and crystallographic environments around the rotor moieties: the central phenylene ring is surrounded by two alkyne groups that provide a negligible electronic barrier for rotation and two outer phenylene rings surrounded by an alkyne and a carboxylate. So, we expect to observe significant differences in dynamics for each component of the linker.[12] To properly observe the gyroscope-like rotation, protons were replaced with deuterons either in the inner ring (**PIZOF-2d_4**, Fig. 1c) or in the outer rings (**PIZOF-2d_8**, Fig. 1c). These two modes of isotopic labeling allowed the isolation of each ring to study of their dynamics by ^{2}H NMR.

Samples of the **PIZOF-2** MOF containing natural and isotopically enriched **PEPEP** links were prepared from adapted published procedures (ESI†).[13] The MOFs were prepared *via* solvothermal crystallization of the respective linkers in DMF in the presence of $ZrCl_4$ and proline-HCl at 120 °C for 24 h, resulting in crystalline powder samples of formula $Zr_6O_4(OH)_4[\text{PEPEP}]_6$, $Zr_6O_4(OH)_4[\text{PEPEP-}d_4]_6$, and $Zr_6O_4(OH)_4[\text{PEPEP-}d_8]_6$. Powder X-ray diffraction (PXRD) patterns of all three isotopologues exhibited sharp diffraction lines starting at 3.84° 2θ (CuKα radiation) characteristic of the cubic **PIZOF-2** MOF phase

($Fd\bar{3}m$ space group symmetry) (Fig. 2a).[14] Phase purity was assessed using Rietveld refinement of the experimental patterns using the single crystal unit cell data resulting in phase pure samples with low residuals (Fig. S1–S4†).

The internal structure of the MOFs was analyzed using ^{13}C Cross-Polarization with Magic Angle Spinning (CP MAS) NMR spectroscopy, where the intensities of ^{13}C signals varied according to the level of deuteration of the linker in each MOF (Fig. 2b). **PIZOF-2** exhibits a ^{13}C spectrum with signals at around 92 ppm, corresponding to the internal ethynyl, signals between 120 and 140 ppm corresponding to the phenylene carbons, and signals at 173 ppm that correspond to carboxylates, consistent with the expected structure. In **PIZOF-2d_4** the signals that correspond to the central phenylene ring are attenuated (Fig. 2b, signal 8) compared to the natural material, whereas in **PIZOF-2d_8**, the only visible signals are those of the central ring, due to the absence of vicinal protons required for CP. Peaks associated with solvents and other reagents were not observed indicating a successfully evacuated framework, which in addition to high crystallinity and the magnetic field produces changes in the spectral line shape that can be associated with
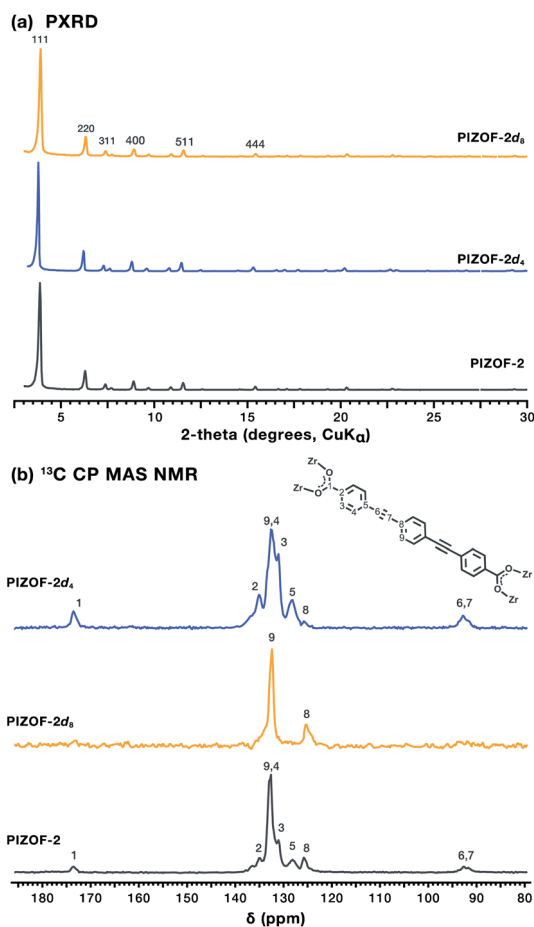

Fig. 2 (a) Powder X-ray diffraction of the natural and isotopically enriched **PIZOF-2** MOFs demonstrating their isoreticular nature. Miller indices of the most intense peaks are indicated. (b) ^{13}C CPMAS NMR spectra of natural and isotopically enriched **PIZOF-2** MOFs.

different types of motion.[15] In the case of the PIZOF MOFs, the differences in the molecular substructure and porosity ensured having optimal samples for dynamic studies. Despite being double interweaved, the distances between centroids of the aromatic rings of the interpenetrating frameworks have values in the range of 6.23 Å to 8.04 Å (Fig. S7†). Considering that the volume of revolution of the phenylene is *ca.* 6 Å, significant changes in the internal rotational dynamics caused by interpenetration were ruled out. Besides, it is expected that the phenylene rings have sufficient space to undergo fast rotational displacement, as it has been observed in other MOFs.[16] To determine this, the deuterated samples were studied using solid-state quadrupolar echo ^{2}H NMR spectroscopy. The reorientation of the C–^{2}H bond vectors with respect to the external between outer and inner rings is expected to afford different rotational rates.

The ^{2}H NMR line shape at room temperature of **PIZOF-2d_8** displays signals characteristic of motions in the intermediate exchange regime. A successful fitting of the spectrum using *NMRweblab*[17] was obtained using a model that assumed twofold flip jumps, indicating a rotational rate at room temperature of the outer rings of $k_{rot} = 2.10$ MHz (Fig. 3 top). The rate of rotation of the deuterated outer rings is similar to that reported in **UiO-66**(Zr)[18] ($k_{rot} = 2.3$ MHz at rt) and much larger than that of other simple MOFs like **MOF-5**(Zn),[12] **MIL-47**(V),[19] and **MIL-53**(Cr)[19] ($k_{rot} < 0.001$ MHz at rt). The rotation of the outer rings could be then regulated by the electronic conjugation of the phenylene with the carboxylates and/or affected by the interactions with the metal oxide clusters.

Conversely, in the case of **PIZOF-2d_4** (Fig. 3 bottom) the narrow ^{2}H NMR spectrum is characteristic of ultrafast reorientations about the –C≡C– axis. A fitting of the spectrum was carried out assuming fast 180° jumps and large amplitude vibrations, indicating a rate of rotation of $k_{rot} > 10$ MHz, the upper limit of the ^{2}H NMR sensitivity, so at 295 K the inner rings are rotating freely. This rate correlates with the minimal electronic barrier given by the flanking alkynes as has also been

observed in a Zn-pyrazolate MOF that contains the same diethynyl-phenylene-diethynyl moiety.[16] To date, this is the first time a MOF exhibits multiple rotational rates of their phenylene rings, which has implications for understanding and improving guest-diffusion related phenomena such as guest storage, catalysis, and separations.

As the transport of guests throughout the MOF would be affected by the interactions between the guest and the static and dynamic components of the framework, we impregnated deuterated **PIZOF-2** samples with tetracyanoquinodimethane (TCNQ). Given the electron-rich nature of the linker, electron deficient TCNQ was selected because it fits into the pores and has a high propensity to form strong π–π stacking bonds, often in the form of charge transfer complexes.[20] In other words, TCNQ is a very sticky molecule known to affect the electronic structure of MOFs and has been used as an additive to enhance their charge conduction properties for device applications.[21,22]

The incorporation of TCNQ into the MOF was performed by immersing MOF powder samples in CH_2Cl_2 solutions for a minimum of 6 h at 295 K followed by rinsing, resulting in a loading capacity of 28.6 ± 0.2 TCNQ molecules per unit cell. At this saturated state, the white crystals changed to a green color and showed a strong EPR signal with $g = 2.0025$ (Fig. S8c†), compared to the pristine MOF. This could be attributed to a charge transfer event that produces organic radicals which overshadows the intrinsic paramagnetism of the zirconia oxoclusters.[23] We also observed a quench of the emission, with a significant change in the quantum yield from $\Phi_F = 8.5\%$ to $\Phi_F < 0.1\%$ (Fig. S8d†). Fluorescence quenching was expected due to the interaction of electron deficient molecules with the conjugated oligo-phenylene-ethynylene linkers that make the MOF emissive.[24]

The ^{13}C CPMAS spectrum of TCNQ loaded **PIZOF-2d_4** not only confirmed the guest within the pores (Fig. S12†), but it also revealed the changes in the chemical environment around the linkers: the appearance of a second carboxylate signal around $\delta = 174$ ppm and a second quaternary carbon signal around $\delta = 128$ ppm, with higher intensities with an increased loading time (Fig. 4a), attributable to the interaction of TCNQ with the outer rings of the PEPEP links, closer to the Zr cluster. Surprisingly, despite the evidence of the diffusion of TCNQ into the MOF, the solid-state ^{2}H NMR spectrum of **PIZOF-2d_4** loaded with TCNQ for 6 h remained unaltered (Fig. 4b). Increasing the impregnation time to 72 h or increasing the temperature to 60 °C resulted in similar line shapes. These results suggest that the guest may have adsorbed near the outer phenylene rings of the linker. To demonstrate this, **PIZOF-2d_8** loaded with TCNQ for 6 h (Fig. 4c) was studied by ^{2}H NMR. Interestingly, the fitting of the ^{2}H line shape indicated slightly faster rotational rates compared to pristine **PIZOF-2d_8**, changing from $k_{rot} = 2.1$ MHz to $k_{rot} = 3.3$ MHz. Only rising the impregnation temperature to 60 °C for 24 h allowed faster adsorption equilibration, decreasing the rotational rate to $k_{rot} = 1.2$ MHz. This indicates that the diffusion of TCNQ is slow and may require longer equilibration times at higher temperature to reach an equilibrium. Furthermore, considering the changes in the chemical shift of the carboxylate peak observed by ^{13}C NMR CP MAS upon the
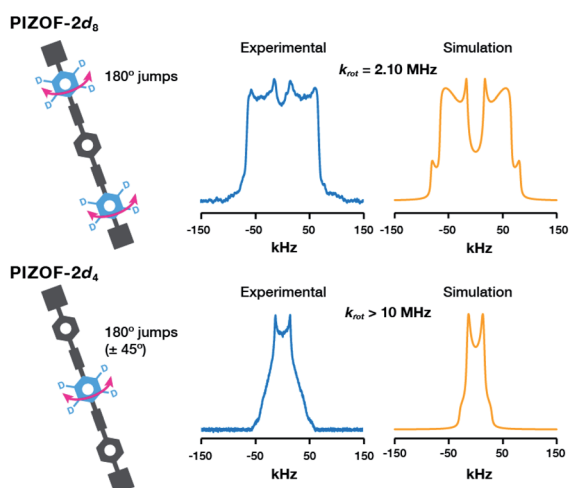

Fig. 3 Experimental (blue) and calculated (orange) deuterium line shapes of PIZOF-2 at 295 K: (top) **PIZOF-2d_8** and (bottom) **PIZOF-2d_4**.
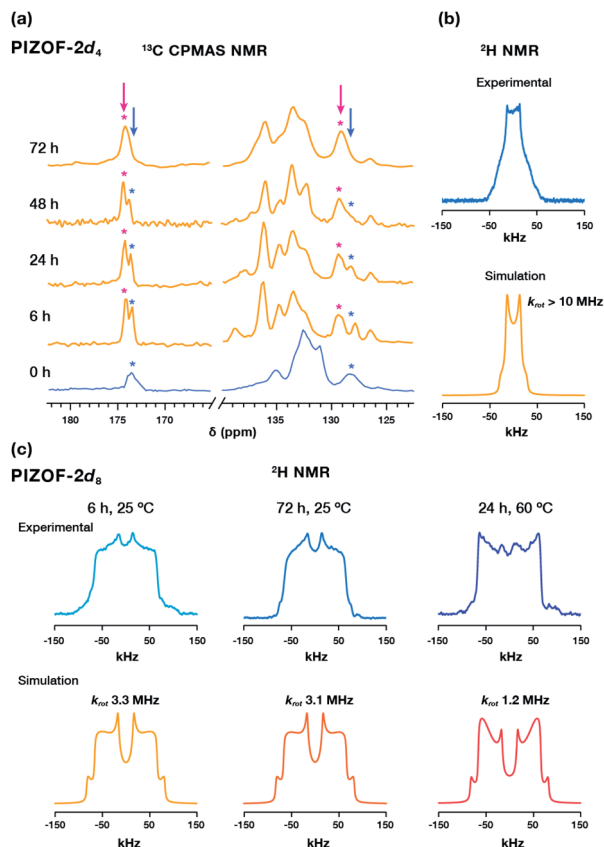
Fig. 4 (a) ^{13}C CPMAS of **PIZOF-2d$_4$** at different TCNQ loading times. (b) Experimental and simulated ^2H NMR spectra of **PIZOF-2d$_4$** revealing that the signal from the central phenylene remains unaffected. (c) Experimental and simulated ^2H NMR of **PIZOF-2d$_8$** under different TCNQ loading conditions.

diffusion of the guest (Fig. 4a, pink mark), as well as the minor changes in the rotational dynamics of the aromatic rings, we postulate that the TCNQ is located closer to the metal cluster, which agrees well with previously observed guest-loaded Zr-based MOFs.[25,26]

This work highlights that our approach can tackle one of the challenges in guest-loaded MOFs, which is the understanding of the interactions between the guest and the framework, a problem often exacerbated by the difficulty of acquiring high-quality single crystals. Furthermore, even after obtaining suitable crystals, X-ray diffraction studies provide only averaged space and time information. Conversely, solid-state NMR, as it is time-resolved, is ideal to analyze guest loaded MOFs in bulk samples, providing kinetic information such as transient π-interaction sites,[27] gas-absorption diffusional rates,[28] internal rotational dynamics,[6] and other kinetic details.[29,30]

Conclusions

In summary, we studied for the first time the amphidynamic behavior of the ultra-stable **PIZOF-2** MOF in the absence and presence of the TCNQ guest through a combined material characterization and solid-state NMR technique using

isotopically enriched linkers. We found that the phenylene rings in the linkers of this MOF exhibit two different rotational rates and that they are not equally affected by the inclusion of the guest. This study offers insights into the complex molecular dynamics within MOFs aiming for tunable properties of synthetic molecular machines. Further work exploring the dynamics of the MOF **PIZOF-2** at different temperatures and the effect of the guest on the rotation under those conditions is currently underway.

Conflicts of interest

There are no conflicts to declare.

Acknowledgements

Notes and references

1 C. S. Vogelsberg and M. A. Garcia-Garibay, *Chem. Soc. Rev.*, 2012, **41**, 1892–1910.
2 A. Colin-Molina, D. P. Karothu, M. J. Jellen, R. A. Toscano, M. A. Garcia-Garibay, P. Naumov and B. Rodríguez-Molina, *Matter*, 2019, **1**, 1033–1046.
3 C. S. Vogelsberg, F. J. Uribe-Romo, A. S. Lipton, S. Yang, K. N. Hou, S. Brown and M. A. Garcia-Garibay, *Proc. Natl. Acad. Sci. U. S. A.*, 2017, **114**, 13613–13618.
4 J. Gonzalez, R. Nandini Devi, D. P. Tunstall, P. A. Cox and P. A. Wright, *Microporous Mesoporous Mater.*, 2005, **84**, 97–104.
5 G. Bastien, C. Lemouchi, P. Wzietek, S. Simonov, L. Zorina, A. Rodríguez-Fortea, E. Canadell and P. Batail, *Z. Anorg. Allg. Chem.*, 2014, **640**, 1127–1133.
6 X. Jiang, H. B. Duan, S. I. Khan and M. A. Garcia-Garibay, *ACS Cent. Sci.*, 2016, **2**, 608–613.
7 A. Gonzalez-Nelson, F. X. Coudert and M. A. van der Veen, *Nanomaterials*, 2019, **9**, 330–336.
8 A. Schaate, P. Roy, T. Preuße, S. J. Lohmeier, A. Godt and P. Behrens, *Chem.–Eur. J.*, 2011, **17**, 9320–9325.
9 R. J. Marshall, Y. Kalinovskyy, S. L. Griffin, C. Wilson, B. A. Blight and R. S. Forgan, *J. Am. Chem. Soc.*, 2017, **139**, 6253–6260.
10 B. Chen, M. Eddaoudi, S. T. Hyde, M. O'Keeffe and O. M. Yaghi, *Science*, 2001, **291**, 1021–1023.
11 M. Eddaoudi, D. B. Moler, H. Li, B. Chen, T. M. Reineke, M. O'Keeffe and O. M. Yaghi, *Acc. Chem. Res.*, 2001, **34**, 319–330.
12 S. L. Gould, D. Tranchemontagne, O. M. Yaghi and M. a Garcia-garibay, *J. Am. Chem. Soc.*, 2008, **130**, 3246–3247.

13 R. J. Marshall, S. L. Griffin, C. Wilson and R. S. Forgan, *Chem.–Eur. J.*, 2016, **22**, 4870–4877.

14 T. L. H. Doan, H. L. Nguyen, H. Q. Pham, N. N. Pham-Tran, T. N. Le and K. E. Cordova, *Chem.–Asian J.*, 2015, **10**, 2660–2668.

15 G. E. Pake, *J. Chem. Phys.*, 1948, **16**, 327–336.

16 S. Bracco, F. Castiglioni, A. Comotti, S. Galli, M. Negroni, A. Maspero and P. Sozzani, *Chem.–Eur. J.*, 2017, **23**, 11210–11215.

17 V. Macho, L. Brombacher and H. W. Spiess, *Appl. Magn. Reson.*, 2001, **20**, 405–432.

18 D. I. Kolokolov, A. G. Stepanov, V. Guillerm, C. Serre, B. Frick and H. Jobic, *J. Phys. Chem. C*, 2012, **116**, 12131–12136.

19 D. I. Kolokolov, H. Jobic, A. G. Stepanov, V. Guillerm, T. Devic, C. Serre and G. Férey, *Angew. Chem., Int. Ed.*, 2010, **49**, 4791–4794.

20 H. Miyasaka, *Acc. Chem. Res.*, 2013, **46**, 248–257.

21 A. A. Talin, A. Centrone, A. C. Ford, M. E. Foster, V. Stavila, P. Haney, R. A. Kinney, V. Szalai, F. El Gabaly, H. P. Yoon, F. Léonard and M. D. Allendorf, *Science*, 2014, **343**, 66–69.

22 M. D. Allendorf, M. E. Foster, F. Léonard, V. Stavila, P. L. Feng, F. P. Doty, K. Leong, E. Y. Ma, S. R. Johnston and A. A. Talin, *J. Phys. Chem. Lett.*, 2015, **6**, 1182–1195.

23 J. Long, S. Wang, Z. Ding, S. Wang, Y. Zhou, L. Huang and X. Wanga, *Chem. Commun.*, 2012, **48**, 11656–11658.

24 D. C. Santra, M. K. Bera, P. K. Sukul and S. Malik, *Chem.–Eur. J.*, 2016, **22**, 2012–2019.

25 A. Van Wyk, T. Smith, J. Park and P. Deria, *J. Am. Chem. Soc.*, 2018, **140**, 2756–2760.

26 A. R. Muguruza, R. F. de Luis, N. Iglesias, B. Bazán, M. K. Urtiaga, E. S. Larrea, A. Fidalgo-Marijuan and G. Barandika, *J. Inorg. Biochem.*, 2020, **205**, 110977.

27 X. Xu, S. Li, Q. Liu, Z. Liu, W. Yan, L. Zhao, W. Zhang, L. Zhang, F. Deng, H. Cong and H. Deng, *ACS Appl. Mater. Interfaces*, 2019, **11**, 973–981.

28 B. E. G. Lucier, S. Chen and Y. Huang, *Acc. Chem. Res.*, 2018, **51**, 319–330.

29 W. Yan, S. Li, T. Yang, Y. Xia, X. Zhang, C. Wang, Z. Yan, F. Deng, Q. Zhou and H. Deng, *J. Am. Chem. Soc.*, 2020, **142**(38), 16182–16187.

30 E. Brunner and M. Rauche, *Chem. Sci.*, 2020, **11**, 4297–4304.